International Journal of Advanced Chemistry, 12 (2) (2024) 51-61

International Journal of Advanced Chemistry

Website: www.sciencepubco.com/index.php/IJET

Research paper

Optimisation of microwave vacuum pyrolysis conversion of palm oil empty fruit bunches into biochar and bio-oil

Ze Wilfrid [1], Musongo Balike [2], Domga Richard [1] *, Obarley Ndip Gilbert [3], Tchatchueng Jean Bosco [1]

[1] *Department of Applied Chemistry, National Advanced School of Agro-Industrial Sciences, University of Ngaoundere, P.O.Box 454 Nga-oundere, Cameroon*

[2] *Department of Chemical Engineering, School of Chemical Engineering and Mineral Industries, University of Ngaoundere, P.O.Box 454 Ngaoundere, Cameroon*

[3] *Department of inorganic Chemistry, Faculty of Science, University of Yaounde I, P.O.Box 337 Yaounde, Cameroon*

**Corresponding author E-mail: domgarichard70@gmail.com*

Abstract

The optimization of the production of Bio-oil and Biochar, from palm oil empty fruit bunches (POEFB) usually thrown as waste, was achieved using microwave vacuum pyrolysis, with expectations of it being a novel source of energy. Moreover, the demand for energy resources is perpetually increasing, due to the rapid increase in population and industrial developments. Surface response methodology via the central composite design was used to investigate the significance of microwave power (w), pyrolysis time (min) and absorbent / biomass ratio (g/g) on the yields in bio-oil and Biochar from POEFB. The optimal yield in bio-oil was 35.05 wt. %, obtained at 14.4 minutes, a ratio of 1: 24 and a power of 382 W and optimum yield in Biochar was 103.75 wt. %, obtained at 1.6 minutes, a ratio of 9:16 and power of 382 W. Thermogravimetric analysis showed the decomposition of hemicellulose at 300 °C, cellulose at 350 °C and lignin from 400 ° C. The greatest effect on the yield in bio-oil from POEFB, was time factor; meanwhile, for the yield in Biochar, the time and absorbent/biomass ratio had the greatest influence.

Keywords: *Biochar; Bio-Oil; Biomass; Microwave Pyrolysis; Optimization.*

1. Introduction

The demand for energy resources is perpetually at an increase, due to the rapid increase in population, urbanization and rapid industrial developments [1]. Fossil energy resources used to satisfy this need involves oil, natural gas and coal. These resources are not only insufficient but are equally non-renewable. Moreover, their pollution effects, especially as bases for atmospheric pollutants, cause irreversible detrimental environmental impacts such as global warming [2-3-4]. Due to the continuous increase in demand and the detrimental environmental impact of these fossil energy sources, the urgent need for an alternative is therefore indispensable [5]. Other sources of energy with more favourable environmental impacts include wind, solar, hydropower and biomass [6].

Biomass is well known as the renewable source of energy capable of meeting up the high demand in energy, as well as, being environmentally friendly [7-8]. Biomass is the third largest primary energy source, after coal and oil [9]. The usage of biomass as a source of energy in developing countries is laudable, given that, agriculture is their principal economic activity [10].

Cameroon is a perfect example of such a developing country, in which, economic policies are essentially oriented towards agricultural development. The development of palm oil production has been of interest, with an estimated production of 465.000 tons in 2020. Cameroon is ranked as the first palm oil producer in the central African region and 12th in the world [11]. SOCAPALM, SAFACAM, SPFS, CDC, PAMOL are some of the companies involved in palm oil production [12]. Production is equally done locally. In both cases, large quantities of agricultural residues, specifically bunches, mostly used as sludge for agricultural applications. Their use for energy production is still to be valorised.

The conversion of Biomasses into energy is a novel field. This conversion is essentially through biochemical or thermochemical processes [13]. Most of these methods apply nitrogen as the vector gas that makes the reaction medium to be inert. This step has been a handicap to researchers in developing countries due to high cost and high maintenance required by the nitrogen plant. To remedy this in our study, we succeeded to create a vacuum pump giving a particularity to the study. Our interest will be on thermochemical methods, specifically microwave pyrolysis, which is efficient in the production of the liquid (Bio- oil) and solid (Biochar). Microwave pyrolysis has been successfully applied on plant residues [14-15]. It is advantageous due to its ability to rapidly transfer heat into the reaction matrix, thus preventing secondary reactions and effectively leading to good yields of products [16]. The pyrolysis is done in an inert environment produced by using a vacuum pump, to absorb oxygen throughout the process. In most cases, nitrogen is used to make the system inert.

In view of this, the main objective of this research is the optimization of the microwave vacuum pyrolysis conversion of empty palm fruit bunches into Bio-oil and Biochar. This is in view of solving the energy problem by developing a new valorisation field; vacuum microwave

Copyright © Ze Wilfrid et al. This is an open access article distributed under the Creative Commons Attribution License, which permits unrestricted use, distribution, and reproduction in any medium, provided the original work is properly cited.

pyrolysis. The current work is structured as follows; A Proximate analysis of the biomass to determine the moisture, ash, fixed carbon and volatile matter content. IR spectroscopic analysis to identify the functional groups present in the sample and thermal decomposition of biomass by thermogravimetric analysis. Eventually, the optimization of the production of the Bio-oil and Biochar by Central Composite Design (CCD). Finally, the bio-oil obtained under optimal conditions was analysed by GC-MS.

2. Material and methods

2.1. Materials

The empty fruits bunches were harvested in December 2016, in a palm grove located in Ebolowa-South Region, Cameroon with Latitude: 2° 54' 59.99" N and Longitude: 11° 08' 60.00" E. They were then sliced into tiny pieces for two weeks to obtain a powder. This powder was left over night in an oven set to 105˚C to remove moisture, which was characterized for proximate parameters, Fourier Transform Infra-Red (FTIR) and Thermogravimetric (TG) analysis. The proximate parameters determined were moisture [17], volatile matter [18], and ash content [19], fixed carbon in the POEFB. FTIR and Thermogravimetric analysis were performed using Perkin Elmer Frontier Spectrometer and Cahn optical microbalance type TG171, respectively.

2.2. Experimental setup

The pyrolytic device is made up of a microwave blender oven with a frequency of 2450 MHz (magnetron), a maximal power of 850 W and time of 35 minutes. The diagram of the modified device used for this study is presented in Fig.1. The microwave cavity was modified to receive the glass reactor made of quartz (0.1 m I.D. × 0.15m height). The condensers connected before and after the oil collector bottle, were cooled by a pump, which supplied them with cold water of temperature between 5 and 10 ° C. The entire installation is inert due to a vacuum system connected via another pump, to the outlet of the gas treatment compartment. This vacuum system allows the rapid evacuation of non-condensable pyrolytic vapours. Thus, limiting side reactions. These non-condensable gases dragged by the vacuum system, passed through the gas-washing device by bubbling and were entrapped.

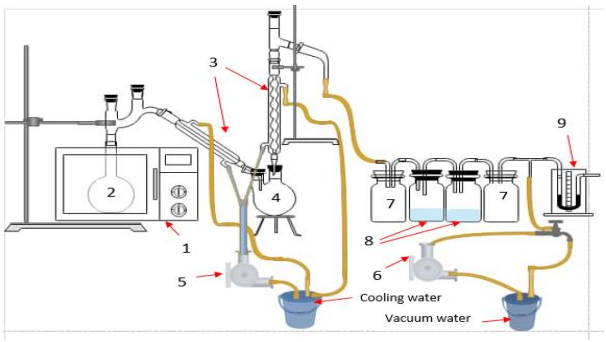

1) Microwave oven,
2) Pyrolysis reactor,
3) Condensers,
4) Oil collector bottle,
5) Cooling pump,
6) Vacuum pump,
7) Guard bottle,
8) Washing bottle,
9) Piezometric tube

Fig. 1: Schematic Diagram of the Pyrolysis System.

2.3. Methods

The pyrolysis process was carried out by introducing into the reactor a reaction mass of 50 g, consisting of biomass powder and biochar (absorbent) in varying proportions. The oil collected in the collection bottle is weighed; the yield of bio oil is obtained from Eq.1. After cooling the reactor, the biochar obtained is weighed and Eq. 2 gives its yield.

$$Bio-oil\ yield\ (\%\ wt) = \frac{Weight\ of\ oil(g)}{Weight\ of\ biomass\ (g)} \times 100 \quad (1)$$

$$Biochar\ (\%\ wt) = \frac{Weight\ of\ biochar(g)}{Weight\ of\ biomass\ (g)} \times 100 \quad (2)$$

Before the optimization of the yield in bio-oil derived from pyrolysis, preliminary studies were carried out in order to define the experimental domains of the parameters influencing these yields. In view of this, 50 g of a sample consisting of a mixture of variable quantities of biochar (wave absorber) [20] and powdered cobs, were introduced into the reactor. To study the influence of a parameter, we varied it and kept the others constant. The parameters studied were the power of the microwave oven (W), the pyrolysis time (min) and the ratio biochar (g) / biomass (g) as follows.

- Effect of the pyrolysis time: the time was varied between 5 to 25 minutes, in intervals of 5 minutes. Meanwhile, the other factors were kept constant (Power 450 W and the ratio 1: 4).
- Effect of the biochar / biomass ratio on pyrolysis: the ratio was varied from 1: 9 to 1: 24. Similarly, the other parameters were kept constant (Power 450 W and Time 10 min)
- Effect of the power on the pyrolysis: the power was varied from 350 W to 750 W, in intervals of 100 W. The time and ratio were kept constant (Time: 10 min, Ratio 1: 4).

The production of bio-oil and biochar were studied using the response surface method via the central composite design; this method makes it possible to reduce the number of experiments, thus, favourable for extending out of the experimental domain using axial points. The responses followed during these experiments were the yields in bio oil and biochar. These factors were in 5 levels called -1, 0, +1, -α, + α and α, depending on the number of parameters in the factorial plane and its value was given by Eq. (3).

$$\alpha = (2k)^{1/4} \quad (3)$$

Where k is the number of parameters studied α= 1.68
The central composite design has been widely used to fit the second-order model and it is advantageous in that, it makes it possible to study the interactions between the factors and to find the optimal conditions. The total number N of experiments needed could be calculated using Eq. (4).

$$N = 2K + 2^K + M \quad (4)$$

Where k is the number of parameters
M is the number of points in the centre.
N = 17 trials
Experimental replications are very necessary because they give the estimated error of the trials carried out.
The second-order polynomial model was developed to obtain an acceptable estimate of the studied responses and to describe the effects of the independent variables. The predicted models to generate the Yi responses (yield of bio-oil and biochar products) were done using Eq. (5).

$$Yi = bo + \sum_{i=1}^{3} b_i X_i + \sum_{i=1}^{3} b_{ii} X_i^2 + \sum_{i=1}^{2} \sum_{j=i+1}^{3} b_{ij} X_i X_j \quad (5)$$

Y_i X_i, b_0, b_i , b_{ii} and b_{ij} are expected response, independent variables, constant coefficient, linear coefficients, interaction and quadratic effects, respectively. This experimental design used 9 coefficients to predict the surface response as described by Eq. (6).

$$Y_i = b_0 + b_1X_1 + b_2X_2 + b_3X_3 + b_{11}X_1^2 + b_{22}X_2^2 + b_{33}X_3^2 + b_{12}X_1X_2 + b_{13}X_1X_3 + b_{23}X_2X_3 \quad (6)$$

Where; X_1, X_2, X_3 are linear effects
X_1^2, X_2^2, X_3^2 are quadratic effects
X_1X_2, X_1X_3, X_2X_3 are interaction effects
b_0, b_1, b_2, b_3 are compensation coefficients and
b_{11}, b_{12}, b_{23} interaction coefficients.
These models were validated by 5 mathematical validation criteria, namely: R^2, R^2 adjusted, the absolute average mean deviation (AAMD) [21], the bias factor (Bf) and the accuracy factor (Af_1) [22]. Their respective equations are given below:

$$\text{AAMD} = \frac{\sum_{i=1}^{p} \left(\frac{|Y_{i\,exp} - Y_{i\,cal}|}{Y_{i\,exp}} \right)}{p} \quad (7)$$

Where Y_{iexp} is the experimental response, Y_{ical} the response calculated from the model for an experiment i and p, the number of experiments.

$$Bf = 10^B \quad (8)$$

Where B is the bias given by Eq. (9).

$$B = \frac{1}{n} \sum log \left(\frac{Y_{i\,exp}}{Y_{i\,cal}} \right) \quad (9)$$

Factors of Accuracies (Af_1).

$$Af_1 = 10^{A_1} \quad (10)$$

With A_1 the accuracy which is determined according to Eq. (11).

$$A_1 = \frac{1}{n} \sum_{i=1}^{n} \left| \log \left(\frac{Y_{i\,exp}}{Y_{i\,cal}} \right) \right| \quad (11)$$

Thus, a model is considered valid if the bias factor, the accuracy factor are equal to 1 and is AAMD equal to zero:

$$Bf = Af_1 = 1 \; and \; 0 < AAMD < 0.3 \quad (12)$$

The STATGRAPHICS Centurion XV.II software was used to perform regression modelling of the yields in bio-oils and biochars. The standard least squares model was used to execute the complete model as described in Eq. (6). The results of the models were analysed statistically and graphically. The global adequacies of the predicted models were checked by the values of the determination coefficients R^2, which provides the percentage of valid model in addition to the previously mentioned criteria. Furthermore, the significance of the high coefficient of determination value was assessed by the Fisher test using the ANOVA table, which is defined as the ratio of the mean square of the regression (CMR) to the experimental error (EE) (F = CMR / EE). The mean square is based on the degree of freedom and the sum of the square of the regression model. The degree of freedom is the number of parameters based on an estimated model and the number of observations. The probability values derived from Table 5 and 6 were compared to probability 0.05, which takes into account the degree of freedom and the level of confidence. For this study, a confidence level of 95 % or a p value ≤ 0.05 was selected for all the experiments. The Sigma Plot software was used to generate the 3-dimensional graphs integrating the 3 parameters, in order to determine the optimal conditions for the production of bio-oils and biochars.
Ash content is the residue obtained after incineration at 550±1ºC. It is determined by the oven method (AFNOR, 1981). Place 5g of sample in a porcelain cup initially dried in the furnace at 550°C and tarred to m, and note the final mass m_1. Place the setup in a furnace at 550±15°C till you obtain a white ash (24h are sufficient). Immediately, place the cup in a desiccator, then measure the mass m_2 of the whole setup when it gets to room temperature. Calculate the ash content as follows:

$$AC = \frac{(m_2 - m)}{(m_1 - m)} x\ 100 \quad (13)$$

The chemical composition of the bio-oil obtained under optimal conditions was analysed by GC-MS of the SHIMADZU brand. The chromatograph used was equipped with a capillary column (5 % Phenyl) - methylpolysiloxane of 30m x 0.25mm x 0.25µm (length x internal diameter x thickness of the stationary phase). The conditions defined for the analysis were as follows: Oven temperature (initial): 60 °C for 3 min, rise to 100 °C at a speed of 3 °C / min, maintain the temperature for 1 min, then rise to 300 °C at a speed of 5 °C / min, hold for 1 min. Helium flow rate: 1.2 mL / min, injector temperature: 300 °C, interface temperature (without division): 225 °C. A volume of 0.4 µL of previously diluted sample at 10 ppm was injected through the heating port of the gas chromatograph. Simultaneously, magnet scanning and data acquisition were started. The mass spectrometer was operated in electronic impact mode (70 eV) over the m / z 50-500 range with a scan speed equal to 1 scan / s. The identification of the compounds resulting from this analysis was carried out using the database of the American National Institute for Standards and Technologies (NIST) internal to the apparatus and a meticulous study of previous scientific literatures.

3. Results and discussion

3.1. Characteristics of the biomass

3.1.1. Determination of ash content

Table 1 presents the results of proximate analysis of the biomass. The moisture content of POEFB was 4.82 %. This result is satisfactory according to the work of Snyder et al. [23], which emphasises that, the moisture content of a lignocellulosic biomass for an efficient production of biofuel must be less than 5 %. A high-water content of the biomass could cause phase separation problems in the bio-oil, as well as, reduce calorific value. In addition, the value found in this study agreed with the work of Siu Hua chang [24], which placed the moisture content values between 2.40 % and 14.28 %. The ash content was 8.96 %. This content as well as the composition, is of paramount importance, because of the minerals present in the pyrolytic charcoal reactions, catalyzed by the biomass. Moreover, after oxidation of the ash, these minerals could cause agglomeration problems in the reactor, during pyrolysis [25]. The obtained ash value, equally agrees with the work of Arshad Adam et al. [26], who found an ash content of 8 %. A high ash content could influence the production of bio-oil but also cause problems of corrosion. According to Fei Yu et al. [27], the problems related to the ash content is more serious when this is higher than 0.1 in bio-oil. The volatile matter and fixed carbon contents are 72.47 % and 13.75 % respectively. These values are found in the reference intervals and are sufficiently high for the biomass to be good for Bio-oil and Biochar production.

Table 1: Characteristics of the Biomass

Characteristics	Values obtained (%)	Reference intervals (%)	References
Moisture content	4.82	2.40 -14.28	
Ash content	8.96	1.30 -13.65	
Volatile content	72.47	70.03 – 83.86	
Fixed carbon content	13.75	8.97- 18.30	[28]

3.1.2. Determination of biomass surface groups by Fourrier Transform IR (FTIR)

The IR absorbance of POEFB are given in Fig. 2. A wide range of functional groups belonging to phenols, alcohols, ketones, aldehydes, alkenes and carboxylic acids are shown these were derived from the decomposition of cellulose, hemicellulose, cellulose and lignin, of the biomass [29].

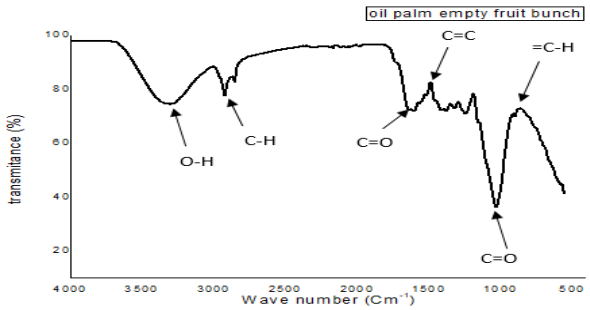

Fig. 2: Infrared Spectra of the EFB Obtained at 500°C.

3.1.3. Determination of the different decomposition phases of x with respect to temperature by thermogravimetric methods

Fig. 3 shows the characteristic phases of the thermal decomposition of biomass. The first phase, is the phase before 400 °C and the second phase, is that found after 400 °C. The first phase appearing from 150 °C, corresponds to the loss of water. The peak at 300 °C characterizes the exothermic decomposition of hemicellulose. This is due to the minor complexity of hemicellulose [30]. The peak at 350 °C characterizes the degradation of cellulose, consisting of molecules composed of long chains of glucose, linked by very rigid hydrogen bonds. This explains its late decomposition [31]. Its reaction is also manifested by a very high mass loss, over a narrow temperature range. The second phase essentially involves the decomposition of the lignin, from 400° C. The complexity of its molecules, explains its degradation over a very wide temperature range [32]. A significant loss in mass is not observed with lignin. This is because it breaks down to favour the production of the Biochar.

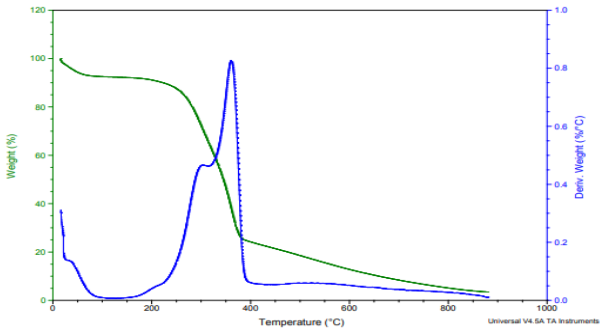

Fig. 3: Thermal Decomposition of POEFB at 500°C.

3.2. Effects of process conditions: determination of experimental domain

In order to determine the appropriate experimental conditions to apply central composite design, preliminary studies were carried out. The influence of each parameter on the yields in Bio-oil and Biochar, were observed. Fig. 4.A below shows the evolution of the bio-oil yield as a function of pyrolysis time. It turns out that the curve had two phases: the first phase, increasing from 5 min to 15 min, with the yield percentages from 14.56 wt.% to 22 wt.% and finally to 30 wt.%. The second phase from 15 min to 25 min, corresponded to a steady state; Phase during which the increase in time no longer influenced the yield in bio-oil. These observations could be explained by the fact that, during the increasing phase, there was a rapid increase in heating thus favouring a rapid destruction of the biomass; That is to say, in this phase, the de-polymerisation and de-fragmentation reactions, leading to the production of the condensable vapours, occurred favourably. The second phase corresponded to the phase during which the secondary cracking arose to produce small gas molecules, slowing down the yield in bio-oil. The optimum reaction time was therefore reached at 15 min. Fig 4.B below, shows the evolution of the yield in bio oil, as a function of the power of the microwave oven. It appears that the maximum yield of 27.45 wt.% was obtained when an irradiation power of 750 W was applied. The increase in the irradiation power led to an increase in heating and accelerated the pyrolytic process. The chemical bonds were quickly broken due to heating. This explained the rapid increase in the bio-oil yield, within the power range of 550 W to 650 W. The influence of the ratio on the bio-oil yield was performed at 450 W, a time set of 10 min and a ratio varied between 1: 9 to 1: 1. Fig 4.C illustrates the variation in bio-oil yield as a function of the absorbent / biomass ratio. It appears that, this yield increased significantly when the absorbent: biomass ratio was varied from 1: 9 to 1: 4, to reach its maximum at this same value of 1: 4 (maximum yield 28.5 wt.%). The increase in yield was due to the small amount of absorbent in the ratio, which allowed better penetration of heat thus enabling the destruction of the structure of the biomass to give the bio-oil. When the absorbent: biomass ratio was varied from 1: 4 to 1: 2, the yield decreased drastically to a minimum of 15 wt.%. The decrease is justified by the fact that, the adsorbent reached its threshold beyond which it could no longer promote rapid absorption of waves in order to produce bio-oil but rather produced charcoal. Table 2 presents the domain chosen for the application of central composite design with the purpose of optimisation.

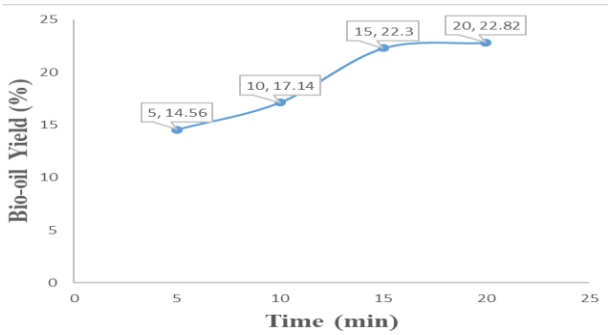

Fig. 4: A. Influence of the Pyrolysis Time on the Bio-Oil Yield.

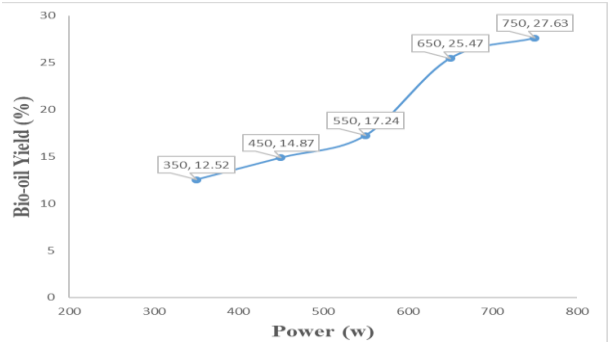

Fig. 4: B. Influence of Power on Bio-Oil Yield.

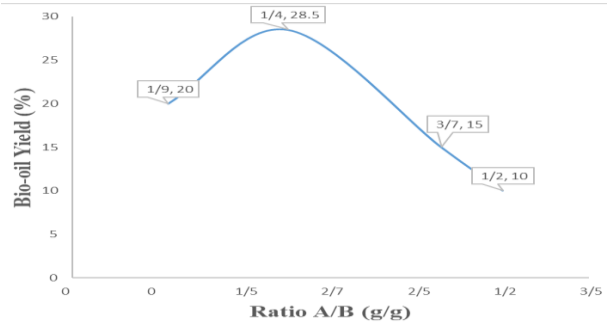

Fig. 4: C. Influence of the Biochar / Biomass Ratio on the Bio-Oil Yield.

Table 2: Values of the Low and High Levels for the 3 Selected Parameters

	Low level		High level	
Parameters	Coded value	Real value	Coded value	Real value
Power (W)	-1	450	+1	650
Time (Min)	-1	5	+1	15
Ratio (absorbent (g)/ biomass(g))	-1	1 : 9	+1	3 : 7

3.3. Optimization process

The surface response methodology provides a fast and reliable method for analysing the conditions of the process and interaction effects. Table 3 presents the experimental matrix of the central composite design in which we have the coded values, the real values, experimental responses, theoretical responses and the residuals of each response .17 experiments were carried out, with 5 levels of parameters.

Table 3: Matrix of the Central Composite Design

N^0	Parameters			Responses	
	X_1 Microwave power (W)	X_2 Pyrolysis time (min)	X_3 Ratio (g/g)	$Y_{Bio-oil}$ (wt.%)	$Y_{Biochar}$ (wt.%)
1	450	5	3:7	15.66	69.22
2	550	10	9:16	27.94	51.06
3	550	1.6	1:4	8.48	64.04
4	650	5	3:7	22.36	68.60
5	382	10	1:4	29.10	44.40
6	550	18.41	1:4	24.48	59.54
7	450	15	3:7	21.70	53.90
8	550	10	1:4	24.22	45.50
9	550	10	1:4	23.88	42.36
10	450	5	1:9	20.06	51.76
11	550	10	1:24	27.96	42.20
12	650	15	3:7	26.60	44.54
13	650	15	1:9	29.16	36.72
14	718	10	1:4	26.42	46.12
15	450	15	1:9	27.86	39.74
16	650	5	1:9	21.22	50.90
17	550	10	1:4	26.20	45.68

3.3.1. Analysis of models

The response to the yields in Bio-oil ($Y_{Bio-oil}$) and Biochar ($Y_{Biochar}$) were tested with respect to the power of the microwave oven (X_1), the time (X_2) and the absorbent / biomass ratio (X_3). The observed responses are given in Table 2. The second order polynomial models for the yields of Bio-oil and Biochar are expressed in Eq.14 and Eq.15 while the Pareto charts for both Bio-oil and Biochar yields is given in Fig. 6.A and B indicating the impact of each of the factors as well as the interactions that result from the study.

$$Y\ Bio\text{-}oil = 24.7971 + 0.699489\ X_1 + 3.87562\ X_2 - 0.879679\ X_3 + 0.859275\ X_1^2 - 0.2075\ X_1\ X_2 + 1.1425\ X_1\ X_3 - 3.12882\ X_2^2 - 0.6825\ X_2\ X_3 + 0.92645\ X_3^2 \quad (14)$$

$$Y\ Biochar = 45.6619 - 0.685907\ X_1 - 2.31006\ X_2 + 2.22897\ X_3 - 0.0304556\ X_1^2 + 3.8375\ X_1X_2 - 5.9625\ X_1\ X_3 + 5.8138\ X_2^2 - 1.8475\ X_2\ X_3 + 0.453914\ X_3^2 \quad (15)$$

Fig. 5.A and B present the calculated and experimental values for the yields of Bio-oil and Biochar. These figures show that the calculated and experimental values are close to each other. The coefficient of determination (R^2) for the Bio-oil yield is 0.9004, which indicates that 90.04 % of the variability of the data is accounted for in the model described in Eq.14. It also indicates that only 9.96 % of the variation in Bio-oil yield data was not explained by the components of the model. The coefficient of determination (R^2) for the Biochar yield is 0.9693, which indicates that 96.93 % of the variability of the data is accounted for in the model described in Eq.15. It also indicates that only 3.07 % of the variation in Biochar yield data was not explained by the components of the model.

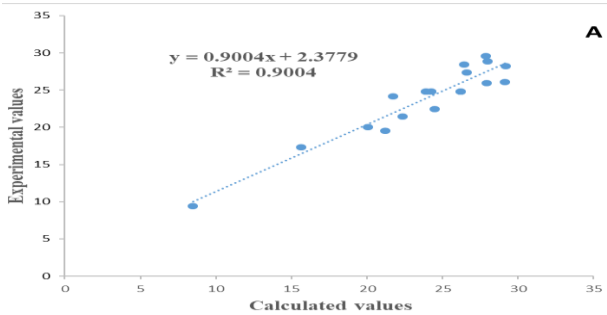

Fig. 5: A Coefficient of Determination of Experimental and Calculated Values of Bio-Oil Yields.

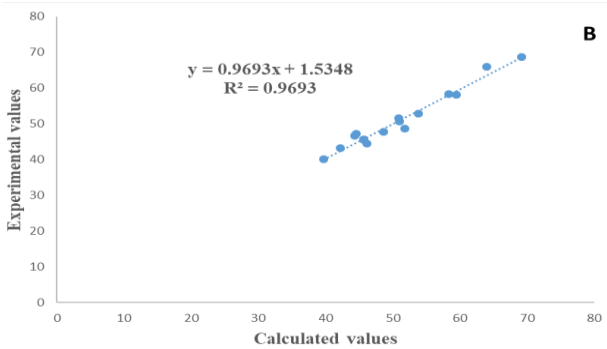

Fig. 5: B Coefficient of Determination of Calculated And Experimental Values of Biochar Yields.

From the model equations, the mathematical validation criteria were determined and recorded in table 4. According to [22], a model is considered valid, if the accuracy and bias are found between 0.75 and 1.25. [21] judge a valid model if the AAMD is between 0 and 0.3. With respect to these references, our models are valid.

Table 4: Model Validation Parameters

Validation indicators	$Y_{Bio-oil}$	B_{iochar}	Validation condition
AAMD	-0.000000017	-0.000000015	0
Bias Factor	1.00117809	0.99998018	1
Accuracy Factor	1.00117809	1.00001982	1
R^2	90.0422	96.92539	≥0,90
R^2 Adjusted	81.0801	94.1581	≥0.80

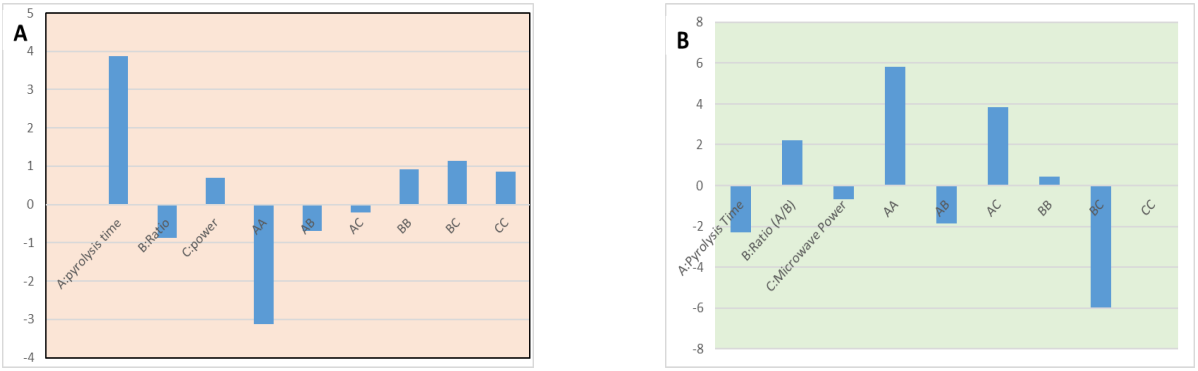

Fig. 6: Pareto Chart for the Modelling of (A) Bio-Oil Yields and (B) Biochar Yield.

The analysis of variances (ANOVA) presented in tables 5 and 6, indicated that, the models observed for the yields of Bio-oil and Biochar gave a good forecast at the confidence level of 95 %, therefore, making it possible to determine the influence of each factor and the degree of significance of their effects. For the Bio-oil yield model, F-value was greater than F-0.05, thus rejecting the null hypothesis. From table 5, only the linear time and quadratic effects of time were significant at 95 % confidence level. On the other hand, for the Biochar yield model in table 6, the significant effects at the 95 % confidence level were the linear effect of time, the linear effect of the ratio and the quadratic effect of time.

Table 5: Analysis of Variance for the Quadratic Bio-Oil Yield Model

Source	Sum of squares	DDL	Quadratic mean	Report F	Proba.
X_1	6.68208	1	6.68208	1.45	0.2562
X_2	205.131	1	205.131	44.52	0.0001
X_3	10.5681	1	10.5681	2.29	0.1609
X_1X_1	10.6406	1	10.6406	2.31	0.1596
X_1X_2	0.34445	1	0.34445	0.07	0.7901
X_1X_3	10.4424	1	10.4424	2.27	0.1631
X_2X_2	141.079	1	141.079	30.62	0.0002
X_2X_3	3.72645	1	3.72645	0.81	0.3897
X_3X_3	12.3693	1	12.3693	2.68	0.1324

Total error	46.0811	10	4.60811
Total (corr.)	462.762	19	

R^2 = 90.0422 % R^2 adjusted = 81.0801 % Standard error of estimate = 2.14665 Average absolute error = 1.34479.

Table 6: Analysis of Variance for the Quadratic Biochar Yield Model

Source	Sum of squares	DDL	Quadratic mean	Report F	Proba.
X_1	6.42511	1	6.42511	1.89	0.1988
X_2	72.8778	1	72.8778	21.49	0.0009
X_3	67.8513	1	67.8513	20	0.0012
X_1X_1	0.013367	1	0.013367	0	0.9512
X_1X_2	117.811	1	117.811	34.73	0.0002
X_1X_3	284.411	1	284.411	83.85	0.0000
X_2X_2	487.103	1	487.103	143.61	0.0000
X_2X_3	27.3061	1	27.3061	8.05	0.0176
X_3X_3	2.96926	1	2.96926	0.88	0.3715
Total error	33.9181	10	3.39181		
Total (corr.)	1103.15	19			

R^2= 96.9253 % R^2 adjusted = 94.1581% Standard error of estimate = 1.84169 Average absolute error = 0.892424

The experiments were conducted to study not only the interactions between the parameters, but also to determine the optimal conditions for the production of Bio-oil and Biochar.

3.3.2. Surface response analysis

Fig. 7.A and B; 8.A and B as well as 9.A and B illustrates the typical surface response to Bio-oil production from palm kernel bunches alongside their corresponding contour iso-response curves. The yield increased with time. A maximum yield of 30 wt.%, occurred at 14 minutes, with the ratio 1:9. fig. 7.C and D; 8.C and D as well as 9.C and D illustrates the surface response to the production of Biochar. It was observed that, the increase in the yield in Biochar, increased with an increment of the absorbent in the ratio. A maximum yield of 48 wt.% occurred at 11 minutes, with the ratio 9:16.

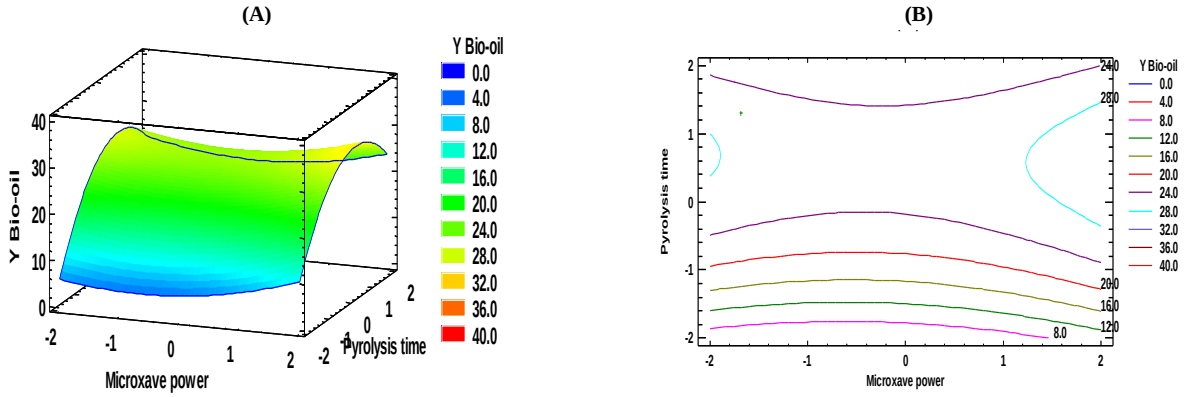

Fig. 7: A and B. Bio-Oil Yield vs Power and Time.

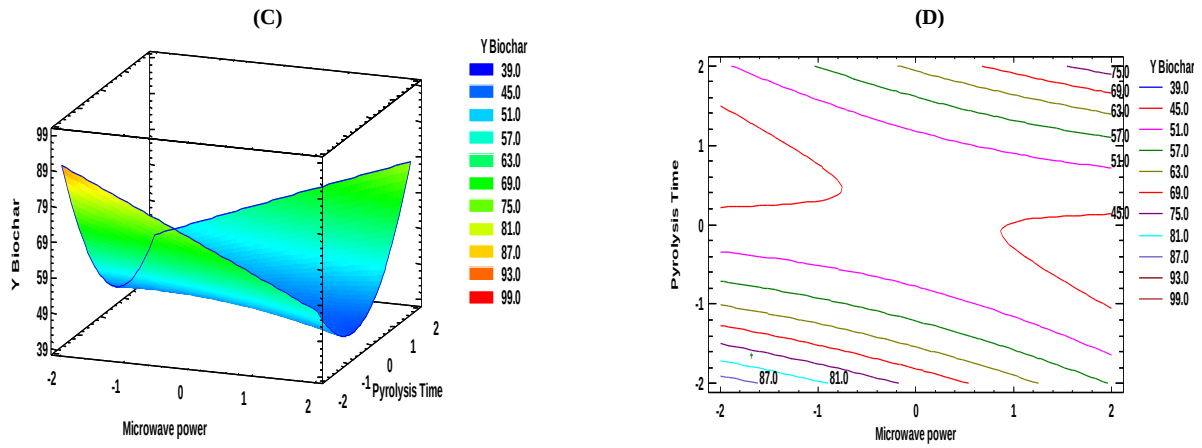

Fig. 7:C and D. Biochar Yield vs Power and Time.

(A) **(B)**

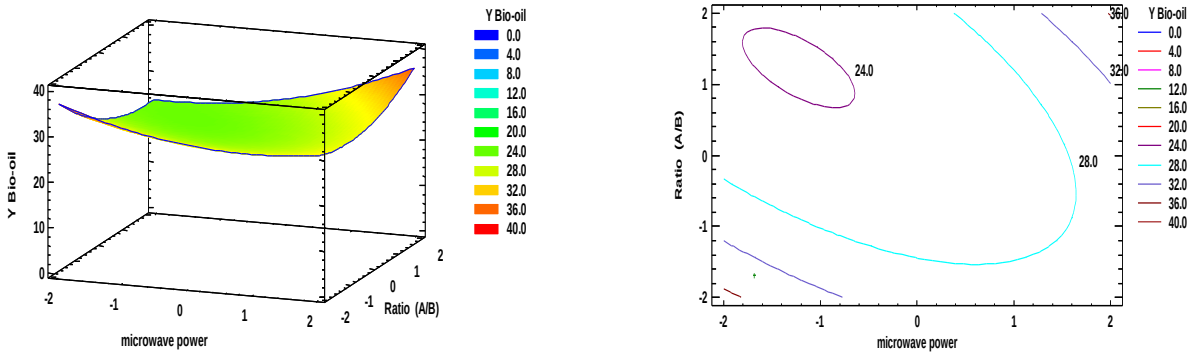

Fig. 8: A and B. Bio-Oil Yield vs Power and Ratio.

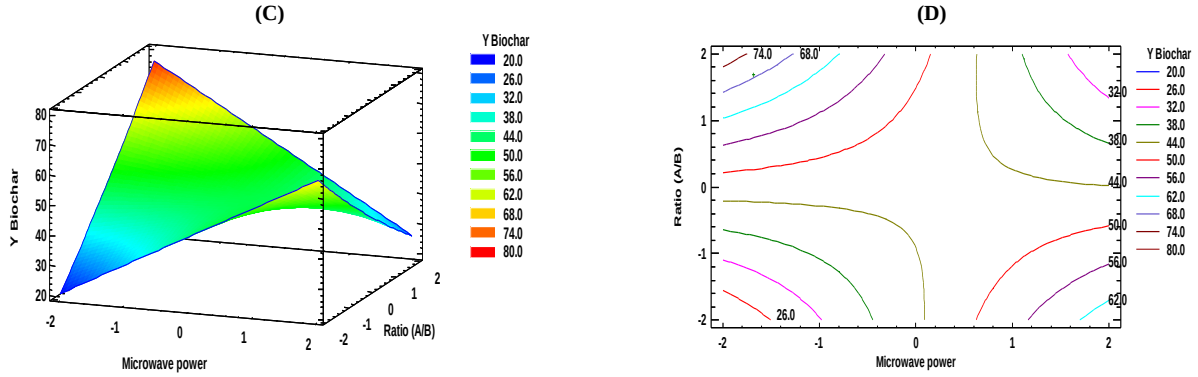

Fig. 8: C and D. Biochar Yield vs Power and Ratio.

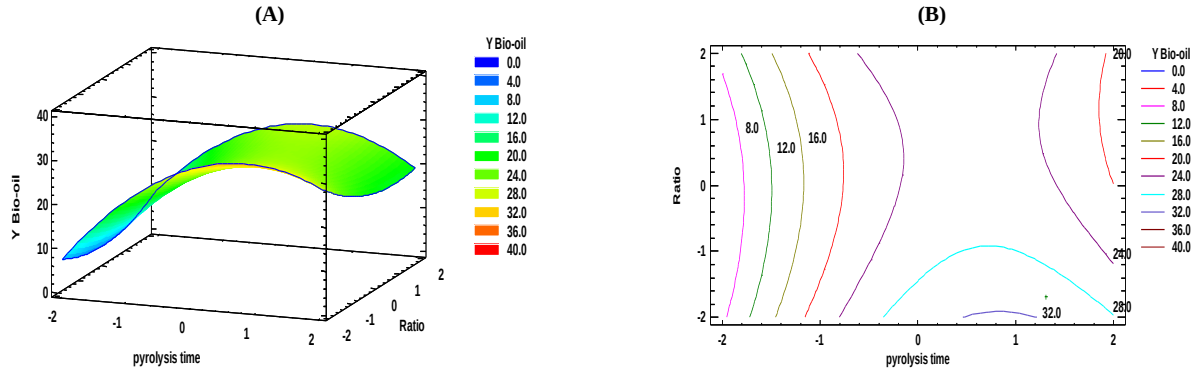

Fig. 9: A and B. Bio-Oil Yield vs Time and Ratio.

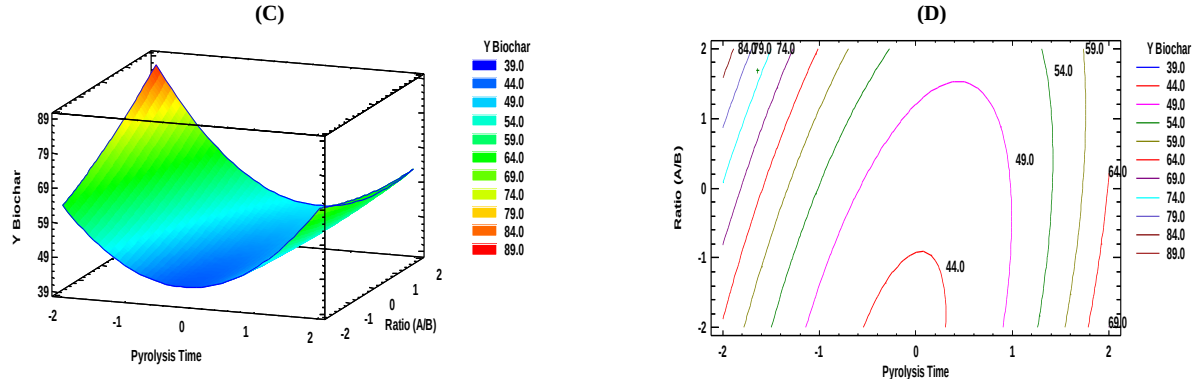

Fig. 9: C and D. Biochar Yield vs Time and Ratio.

3.3.3. Optimum predictions

In order to obtain maximal Bio-oil, a microwave power of 382W needs to be applied for 14.4 Minutes and a ratio of 1:24 in order to obtain an optimum yield of 35.05 % (table 7) while an optimum Biochar yield of 103.75 % is obtained in 1.6 minutes of pyrolysis time and a ratio of 9:16 for a microwave power of 382 W as seen in table 7.

Table 7: Predicted Optimum for Bio-Oil and Biochar Yields

	Y Bio-oil	Y Biochar
Microwave power	382	382
Pyrolysis Time	14.4	1.6
Ratio (A/B)	1:24	9:16
Optimum (%)	35.05	103.75

3.4. Determination of chemical composition of bio-oil

Table 8: Chemical Compounds of Bio-Oil According to GC-MS Analysis

N^{O}	R. T	Area (%)	Identified compounds	Formula	IK
1	9.613	4.54	4-Methoxyphenol	$C_8H_{10}O_3$	1258
2	15.611	0.34	Pentadecane	$C_{15}H_{32}$	1500
3	17.201	4.22	Diethyl phthalate	$C_{16}H_{30}O_4$	1571
4	19.966	0.65	Propyl phthalate	$C_{17}H_{36}$	1701
5	20.591	1.54	Tetradecamethyl heptasiloxane	$C_{14}H_{44}O_6Si_7$	1748
6	21.427	62.17	Diisobutyl phthalate	$C_{16}H_{22}O_4$	1812
7	23.272	1.99	Hexadecanoic acid	$C_{16}H_{32}O_{16}$	1953
8	23.592	0.65	Eicosamethylcyclodecasiloxane	$C_{20}H_{60}O_{10}$	1977
9	23.901	1.09	Eicosane	$C_{20}H_{46}$	2002
10	24.959	0.38	Abieta-8 (14), 9 (11), 12-triene	$C_{20}H_{30}$	2156
11	26.643	0.99	Succinic acid, di (2-octyl) ester	$C_{20}H_{38}O_4$	2401
12	26.732	1.07	Succinic acid, 2-ethylhexyl undecyl ester	$C_{23}H_{44}O_4$	2414
13	28.373	5.28	Heptacosane	$C_{27}H_{56}$	2652
14	28.851	0.36	Glutaric acid, di (3-octyl) ester	$C_{21}H_{40}O_4$	2721
15	29.16	0.42	n.d		2766
16	30.134	3.19	Nonacosane	$C_{29}H_{60}$	2908
17	30.791	0.71	Adipic acid, 2-ethylhexyl tetradecyl ester	$C_{28}H_{54}O_4$	3000
18	31.504	4.9	Methyl Triacontane	$C_{31}H_{64}$	3003
19	33.13	1.99	Benzonitrile, m-phenethyl-3- (2Phenylethyl) benzonitrile 1- (3-Cyanophenyl) -2-phenylethane	$C_{15}H_{13}N$	3100
20	33.329	0.63	Adipic acid, 2-decyl octyl ester	$C_{24}H_{46}O_4$	3321
21	37.288	0.61	3,7,11-trimethyl-2,6,10-dodecatrienoic methyl ester	$C_{17}H_{28}O_2$	3348

Obtained at Power of 450 w, Time of 14 min, Ratio A/B of 1: 9. T.R: Retention time, I.K: kovat index, n.d: not determined.
Table 8 presents the chemical compounds identified in the bio-oil. From the table, the chromatographic analysis carried out revealed the bio-oil consisting mainly of oxygenated compounds (methoxyphenol, diisobutyl phthalate, hexadecanoic acid and aromatic compounds), saturated (alkanes) and unsaturated hydrocarbons (alkenes). This is confiremed by the Kovat index values that match to the corresponding compound using a standard mixture of n-alcanes(C10-C44) fournished by SUPELCO as the reference solvent. This bio-oil is highly rich in esters. Esters constitute about 77.94 % of the overall composition of the bio-oil, of which, 62.17 % is made of diisobutyl phthalate. Diisobutyl phthalate is the highest chemical constituent in the bio-oil. Meanwhile, the unsaturated hydrocarbons have a composition of just 19.78 %. The presence of diisobutyl phthalate in these aromatic and oxygenated compounds was attributed to the biopolymer textures, such as that of, cellulose and hemicellulose [33].

4. Conclusion

In this study, the optimization of the production of Bio-oil and Biochar was achieved through microwave vacuum pyrolysis of POEFB. It was observed that, the biomass was good for the production of Bio-oil and Biochar due to its high content in volatile matter (72.47 %) and fixed carbon (13.75 %), in addition to the presence of biopolymers such as, hemicellulose, cellulose, and lignin, which decomposed respectively at 300 °C, 350 °C and at 400 °C for the yield of the two products. The IR predicted the predominance of functional groups consisting oxygen such as O-H, C = O and C-O in biomass. The time * A / B ratio interactions were solely the most significant in the two models that were developed. The optimum for Bio-oil was 35.05 wt.%, obtained at 14.4 min, ratio of 1: 24 and at a power of 382 W. Meanwhile, the optimum for Biochar was 103.75 wt.%, obtained at 1.6 min, ratio of 9:16 and at a power of 382 W. The results of the GC-MS of bio-oil confirmed the strong presence of aromatic and oxygenated compounds such as diisobutyl phthalate, with a specific area of 62.17%. This was an indicator of the high energy potential of the bio-oil, which could be improved by using more suitable catalysts, in addition to be a large reserve of chemical compounds.

Acknowledgements

The authors wish to hereby acknowledge the Laboratory of Chemical Engineering and Processes (LCEP) of the National Advanced School of Agro-Industrial Sciences, University of Ngaoundere, Cameroon for providing a conducive technical support for the experiments. This research did not receive any specific grant from funding agencies in the public, commercial, or not-for-profit sectors.

References

[1] A. Srivastava, R. Prasad, Triglycerides-based diesel fuels, Re-newable and Sustainable Energy Reviews, 2000, 4 (2), 111-133. https://doi.org/10.1016/S1364-0321(99)00013-1.
[2] Q. Bu, H. Lei, S. Ren, L. Wang, J. Holladay, Q. Zhang, J. Tang, R. Ruan, Phenol and phenolics lignocellulosic biomass by catalytic microwave pyrolysis, Bioresour Technol, 2011, 102 (13), 7004−7007. https://doi.org/10.1016/j.biortech.2011.04.025.
[3] Fressoz, J.-B., La longue marche de la crise écologique, in Ma-nuel d'Histoire critique, 2014, Paris, France. p. 176-177.
[4] Robin, M., Au Dakota du Nord, les vaches perdent leur queue, Le Monde Diplomatique, 2013, 713, 22-23.

[5] R. H. Moss, J. A. Edmonds, K. A. Hibbard, M. R. Manning, S. K. Rose, D. P. van Vuuren, T. R. Carter, S. Emori, M. Kainuma, T. Kram, G. A. Meehl, J. F. B. Mitchell, N. Nakicenovic, K. Riahi, S. J. Smith, R. J. Stouffer, A. M. Thomson, J. P. Weyant, T. J. Wil-banks, The next generation of scenarios for climate change research and assessment, Nature, 2010, 463 (7282), 747−756. https://doi.org/10.1038/nature08823..

[6] EIA, 2012, Annual Energy outlook 2012, USA, Energy Infor-mation Administration. http://www.eia.gov/forecasts/aeo.

[7] A. Bridgwater, G. Peacocke, Fast pyrolysis processes for bio-mass, Renew Sustain Energy Rev, 2000, 4, 1–73. https://doi.org/10.1016/S1364-0321(99)00007-6.

[8] G.W. Huber, S. Iborra, A. Corma, Synthesis of transportation fuels from biomass: Chemistry, catalysts, and engineering, Chem. Rev, 2006, 106, 4044–4098. https://doi.org/10.1021/cr068360d.

[9] A.J. Ragauskas, C.K. Williams, B.H. Davison, G. Britovsek, J. Cairney, C.A. ECKERT, The path forward for biofuels and bio-materials, Science, 2006, 311, 484-489 https://doi.org/10.1126/science.1114736.

[10] A. Madi, Analyse des politiques agricoles en Afrique Subsa-harienne, Note de cours de politique agricole, (2011), Faculté d'Agronomie et des Sciences Agricoles, Département d'Economie Rurale, Université de Dschang, Cameroun.

[11] Index Mundi. Ranking of the top 20 palm oil producing coun-tries. [consult in January 2021]. http://www.indexmundi.com.

[12] L. Feintrenie, 2013, Opportunities to responsible land-based investment practices in Central Africa, World Bank conference on land and poverty, Washington DC, USA, 8-11 April.

[13] A. Demirbas, Global renewable energy resources, Energy Sources Part A Recovery Util. Environ. Eff, 2006, 28, 779–792. https://doi.org/10.1080/00908310600718742.

[14] X. Wang, H. Chen, K. Luo, J. Shao, H. Yang, the influence of microwave drying on biomass pyrolysis, Energy Fuels, 2008, 22, 67–74. https://doi.org/10.1021/ef700300m.

[15] Y.F. Huang, W.H. Kuan, S.L. Lo, C.F. Lin, Hydrogen-rich fuel gas from rice straw via microwave-induced pyrolysis. Biore-sour. Technol. 101, 2010, 1968–1973. https://doi.org/10.1016/j.biortech.2009.09.073.

[16] J. P. Robinson, R. Omar, Conventional and microwave-assisted pyrolysis of rapeseed oil for bio-fuel production, J. Anal. Appl. Pyrol, 2014, 105 131-142 https://doi.org/10.1016/j.jaap.2013.10.012.

[17] ASTM E1756 - 08, Standard Test Method for Determination of Total Solids in Biomass. West Conshohocken, PA: ASTM In-ternational; 2015.

[18] ASTM E872 - 82, Standard Test Method for Volatile Matter in the Analysis of Particulate Wood Fuels. West Conshohocken, PA: ASTM International; 2013.

[19] ASTM E17551 - 01, Standard Test Method for Ash in Bio-mass. West Conshohocken, PA: ASTM International; 2015.

[20] A. Dominguez, Y. Fernandez, B. Fidalgo, J.J. Pis, J.A. Menendez, Bio-syngas Production with low concentrations of CO2 and CH4 from microwave-induced pyrolysis of wet and dried sew-age sludge. Chemosphere, 2008, 70, 393-403 https://doi.org/10.1016/j.chemosphere.2007.06.075.

[21] D. Bas, I.H. Boyac, Modeling and optimization: Usability of response surface methodology, Journal of Food Engineering, 2007, 78, 836-845. https://doi.org/10.1016/j.jfoodeng.2005.11.024.

[22] F.P.M. Rodriguez, Méthodologie expérimentale et optimisation des Formes pharmaceutiques pour application locale, L.T. DOC, Editor Paris,1996, 237-273.

[23] S.H. Chang, An overview of empty fruit bunch from palm oil as feedstock for bio-oil production, Biomass and Bioenergy, 2014, 62, 174-181 https://doi.org/10.1016/j.biombioe.2014.01.002.

[24] M. Gupta, L.W. Wong, Eugene, Microwaves and metals, John Wiley & Sons (Asia), 2007 https://doi.org/10.1002/9780470822746.

[25] A.A Salema, F.N. Ani, Microwave pyrolysis of palm oil fibres, Journal Mekanikal No.30, 2010, 77-86.

[26] F. Yu, S. Deng, R. Ruan., Physical and chemical properties of bio-oils from microwave pyrolysis of corn stover, Applied Bio-chemistry and Bio-technology, 137–140 (1–12), 2007, 957–970. https://doi.org/10.1007/s12010-007-9111-x.

[27] S. Kerdsuwan, k. Laohalidanond, Renewable energy from palm oil empty fruit bunch. In: Nayeripour M, editor. Renewable energy: trends and applications. Shanghai: Intech, 2011, 123-50 https://doi.org/10.5772/25888.

[28] Q. Zhang, J. Chang, T. Wang, Y. Xu, Review of biomass pyrolysis oil properties and upgrading research, Energy Conversion and Management, 48 (1), 2007, 87–92. https://doi.org/10.1016/j.enconman.2006.05.010.

[29] G. Almeida, J.O. Brito, P. Perre, Alterations in energy properties of eucalyptus wood and bark subjected to torrefaction : The potential of mass loss as a synthetic indicator. Bioresource Technology, 101, No 24, 2010, 9778-9784. https://doi.org/10.1016/j.biortech.2010.07.026.

[30] P. Rousset, C. Lapierre, B. Pollet, W. Quirino, P. Perre, Effect of severe thermal treatment on spruce and beech wood lignins. Annals of Forest Science, 66, No 1, 2009, 110. https://doi.org/10.1051/forest/2008078.

[31] H. Yang, R. Yan, H. Chen, D. H. Lee, C. Zheng, Characteristics of Hemicellulose, Cellulose and Lignin Pyrolysis, Fuel, 86 (12–13), 2007, 1781–1788. https://doi.org/10.1016/j.fuel.2006.12.013.

[32] W.T. Tsai, M.K. Lee and Y.M. Chang, Fast pyrolysis of rice straw, sugarcane bagasse and coconut shell in an induction-heating reactor. J. Anal. Appl. Pyrol., 76, 2006, 230-237. https://doi.org/10.1016/j.jaap.2005.11.007.